

Mechanisms for electron transport in atomic-scale one-dimensional wires: soliton and polaron effects

H. Ness * and A.J. Fisher †

*Department of Physics and Astronomy, University College London,
Gower Street, London WC1E 6BT, U.K.*

We study one-electron tunneling through atomic-scale one-dimensional wires in the presence of coherent electron-phonon (e -ph) coupling. We use a full quantum model for the e -ph interaction within the wire with open boundary conditions. We illustrate the mechanisms of transport in the context of molecular wires subject to boundary conditions imposing the presence of a soliton defect in the molecule. Competition between polarons and solitons in the coherent transport is examined. The transport mechanisms proposed are generally applicable to other one-dimensional nanoscale systems with strong e -ph coupling.

PACS numbers: 73.63.Nm, 73.40.Gk, 73.61.Ph

I. INTRODUCTION

How will an electronic system conduct in the limit where it becomes entirely one-dimensional? This became an issue in the late 1980s, with the fabrication of semiconductor structures that possessed only a single conducting “channel”, and which exhibited the phenomenon of quantized conductance [1]. With nanoscale fabrication techniques, the class of effectively one-dimensional systems has expanded to include: atomic-scale structures on surfaces produced by scanning probe lithography [2], self-assembly [3], or directed assembly [4]; break junctions [5,6]; carbon nanotubes [7]; and conjugated organic molecules [8]. The measurement of the transport properties of individual examples of such systems is now possible; for example, conduction in individual molecules has recently been measured by scanning probes [9,10] or bulk electrodes [8,11]; transport in nanotubes has been measured using lithographed electrodes [12]. Similar measurements may also soon become possible for atomic-scale wires on surfaces.

Many of these recent examples approach the ideal of a system whose atomic—as well as electronic—structure is truly one-dimensional. As such they may be expected to exhibit enhanced effects of correlations during electron transport. Electron-electron correlations have consequences including the possible formation of Luttinger liquids [13]; on the other hand, the effects produced by electron-atom correlations can include the Peierls transition [14], which opens a gap at the Fermi energy and renders one-dimensional metallic systems semiconducting. If these quasi-one-dimensional systems are to have applications in nanotechnology, it is vital to understand whether currents can pass through them, despite the possibility

of a Peierls transition. In this paper we address this question, in the context of molecular wires; specifically, we consider finite-length poly-acetylene chains described by a fully quantum version of the Su–Schrieffer–Heeger (SSH) model [15].

We have chosen to study molecular conductors here, rather than any of the other types, because electron-lattice coupling in bulk samples is relatively well studied [15]. The Peierls transition manifests itself in an alternation of single and double bonds (i.e., *dimerisation*) along the molecule’s length, and bulk electron transport is dominated by mobile intrinsic defects formed when electrons or holes are injected into this dimerised structure. For our purposes the most important defects are polarons (which can be thought of as a local reduction in the dimerisation around an injected charge) and charged solitons (topological defects in the bond length alternation). The soliton has an associated electronic state at mid-gap and the dimerisation changes sign, passing through zero in the neighbourhood of the defect [15].

In order to understand molecular charge transport on nanometre lengthscales, we must develop a theory of coherent transport that accounts for polaron and soliton formation. We took the first steps recently when we showed that the tunneling of carriers through molecular wires at low temperature is dramatically enhanced by the formation of virtual polarons [16]. Therefore, previous treatments of tunneling in molecules based on elastic scattering significantly underestimate the conductance [17]. However, the boundary conditions used in our previous work prevented solitons from forming in the molecule, as the dimerisation was constrained to be equal at both ends. In the present paper we study chains with an odd number of monomers; the ground state of such a

* Present address: CEA-Saclay, DSM/DRECAM/SPCSI, Bât. 462, F-91191 Gif-sur-Yvette, France. E-mail: ness@cea.fr

† E-mail: Andrew.Fisher@ucl.ac.uk

system possesses a single soliton in the centre [15,18]. We are thus able to study for the first time the role of the moving soliton, with its associated mid-gap state, and the competition between polarons and solitons in coherent transport.

II. PHYSICAL MODEL

The model for the molecular wires includes delocalized π -electrons interacting with quantum phonons. The electronic Hamiltonian is expressed in the basis of the one-electron eigenstates (labelled by n, m) of the reference system. The e -ph coupling is linear in the phonon displacements and induces transitions between electronic states. The molecule Hamiltonian is

$$H = \sum_n \epsilon_n c_n^\dagger c_n + \sum_\lambda \hbar\omega_\lambda a_\lambda^\dagger a_\lambda + \sum_{\lambda, n, m} \gamma_{\lambda nm} (a_\lambda^\dagger + a_\lambda) c_n^\dagger c_m, \quad (1)$$

where c_n^\dagger (c_n) creates (annihilates) an electron in the n -th electronic state with energy ϵ_n and a_λ^\dagger (a_λ) creates (annihilates) a quantum of energy $\hbar\omega_\lambda$ in the eigenmode of vibration λ of the isolated molecule. The values of ϵ_n , ω_λ and $\gamma_{\lambda nm}$ are calculated from the ground state of the neutral molecule (described by the SSH model [15,16]) containing an odd number N of monomers. The vibrational eigenmodes V_λ and frequencies of the molecule are calculated within the harmonic approximation [19].

To calculate the transport properties through the wire, the left and right ends of the molecule (atomic sites $i = 1$ and $i = N$) are connected to metallic leads via hopping integrals $v_{L,R}$ respectively. The leads are modeled as one-dimensional semi-infinite tight-binding chains with on-site energy $\epsilon_{L,R}$ and inter-site hopping matrix elements $\beta_{L,R}$ (with no e -ph coupling). The scattering states $|\Psi\rangle$ for a single incoming charge carrier are expanded inside the molecule onto the eigenstates $|n, \{n_\lambda\}\rangle = c_n^\dagger \prod_\lambda (a_\lambda^\dagger)^{n_\lambda} / \sqrt{n_\lambda!} |0\rangle$, of the non-interacting e -ph system¹. n_λ is the occupation number of the phonon mode λ and $|0\rangle$ is the *vacuum* state (representing the neutral ground state of the whole system,

with a definite number of electrons in each part). The single added carrier can be anywhere in the system (on the left, the right, or in the molecule) and interacts with phonons only when inside the molecule. We only consider current-carrying states in which a single electron is added to the ground state; we expect this assumption to hold since the interval between electron transmission is much greater than the transit time [16].

We now briefly outline the calculation technique. The transport problem is solved by mapping the many body (one-electron/many-bosons) problem onto a single-electron problem with many scattering channels [20,16]. Each channel represents the different scattering processes by which the electron might exchange energy with the phonons. For an initial phonon distribution $b \equiv \{m_\lambda\}$ and an incoming electron from the left lead, the outgoing channels in the left and right leads are associated with energy-dependent reflection $r_{ab}(\epsilon)$ and transmission $t_{ab}(\epsilon)$ coefficients respectively ($a \equiv \{n_\lambda\}$ is the phonon distribution after scattering in each outgoing channel). In the leads, the scattering states take the asymptotic form of propagating Bloch waves with amplitudes r_{ab} (reflection) and t_{ab} (transmission). The wave vectors are given by the dispersion relations in each channel. For example, the energy ϵ_{in} of the incoming electron from the left lead is related to the wave vector k_b^L by the tight-binding-like dispersion relation $\epsilon_{in} = \epsilon_L + 2\beta_L \cos k_b^L$. For the final energy ϵ_{fin} of the electron transmitted to the right, one has: $\epsilon_{fin} = \epsilon_R + 2\beta_R \cos k_a^R$. One can then project out the leads from the problem and work in the molecular wire subspace to solve for the value of the scattering state $|\Psi(E)\rangle$. This state is obtained from propagating the source term $|s(E)\rangle$ (incoming electron from the left) via the effective Green's function $G(E)$ defined in the molecular wire subspace: $|\Psi(E)\rangle = G(E)|s(E)\rangle$, where G is given by $G(E) = [E - H - \Sigma_L(E) - \Sigma_R(E)]^{-1}$, H is the molecular wire Hamiltonian defined in Eq. (1) and $\Sigma_{L,R}(E)$ are complex potentials arising from embedding the molecular wire spectrum into the continuum of states associated with the leads. Overall energy is conserved, so ϵ_{in} and ϵ_{fin} are related by: $E = \epsilon_{in} + \sum_\lambda m_\lambda \hbar\omega_\lambda = \epsilon_{fin} + \sum_\lambda n_\lambda \hbar\omega_\lambda$ ².

The linear system $|\Psi\rangle = G|s\rangle$ is solved for a finite size

¹ A similar expansion is used in the leads, c_n^\dagger is then replaced by the charge creation operator d_i^\dagger on site i .

² In this paper, we consider the limit of low temperatures: the initial phonon distribution is $b \equiv \{m_\lambda\} = \{0\}$ where all optic phonon modes are in the ground state (in this limit, the injection energy equals the total energy $\epsilon_{in} = E = \epsilon_{fin} + \sum_\lambda n_\lambda \hbar\omega_\lambda$). It is a very good approximation even at room temperature for all optic modes except the soliton translation. For the soliton translation the condition $kT \ll \hbar\omega$ restricts us to $T \ll 230K$.

basis set by truncating the phonon subspace (*i.e.* considering the lowest occupation numbers up to $n_{\text{occ}}^{\text{max}}$ in each mode). Furthermore the electron is coupled inside the molecule to a finite number N_{ph} of the most relevant phonon modes (see next section). A detailed analysis of the validity of such approximations can be found in Ref. [16]. From the solution $|\Psi\rangle = G|s\rangle$, one can obtain the reflection r_{ab} and transmission t_{ab} coefficients for all the channels and hence the currents flowing through the wire. One can also calculate the expectation values of any *correlation functions* between the electron and phonon degrees of freedom.

We define the transmission probability $T_{ab} = |t_{ab}(\epsilon_{in})|^2 \beta_R \sin k_a^R(\epsilon_{fin}) / (\beta_L \sin k_b^L(\epsilon_{in}))$ ³. In our model, $|t_{ab}|^2$ is proportional to $|\langle i = N, a | \Psi \rangle|^2 = |\langle N, a | G | s \rangle|^2$ and the source term is proportional to the velocity of the incoming electron [16]. Then, working in the real-space representation, the inelastic transmission probability can be rewritten in the following usual form [21]:

$$T_{ab}(\epsilon_{fin}, \epsilon_{in}) = 4 \frac{v_L^2}{\beta_L} \sin k_b^L(\epsilon_{in}) \frac{v_R^2}{\beta_R} \sin k_a^R(\epsilon_{fin}) \times |\langle i = N | G_{ab}(E) | i = 1 \rangle|^2, \quad (2)$$

where $\langle N | G_{ab}(E) | 1 \rangle$ is the matrix element of the Green's function G taken between the left side $i = 1$ and the right side $i = N$ of the molecule and the phonon configurations before (b) and after (a) scattering⁴.

III. RESULTS

First we describe the vibrational modes needed to obtain the relevant distortions of the molecule. We have shown that polaron formation inside the molecule after charge injection is due to the coupling to the long-wavelength optic modes [16]. For odd-number chains where a soliton defect is present, we have to include in addition the modes responsible for the motion and the deformation of the soliton. We therefore include the soliton translation (the 'Goldstone mode'), the 'amplitude mode' related to the deformation of the soliton width, and higher-order deformation modes (for example the so-called third mode) [15,22]. Figure 1 shows the phonons

considered for a molecule of length $N = 99$. As an illustrative example, we also show in Fig. 2 the dimerisation d_j for neutral isolated even- and odd-length molecules. The dimerisation is obtained, in terms of atomic displacements u_j , from the staggered difference between adjacent bond lengths: $d_j = (-1)^j (u_{j+1} - 2u_j + u_{j-1})$. For even N , the neutral molecule is perfectly dimerized: the dimerisation d_c is constant in the middle of the chain despite the end effects. For odd N , a soliton appears in the middle of the chain, acting as a domain wall separating the two domains of opposite sign of dimerisation.

Now we turn on the lattice deformations induced by electron propagation in the (odd N) molecule connected to the electrodes⁵. The lattice deformations induced by the tunneling electron are given by the correlation function $\delta_\lambda^{[i]}$ between the electron density $P_i = c_i^\dagger c_i$ on site i and the displacement $\Delta_\lambda = (a_\lambda + a_\lambda^\dagger) \sqrt{\hbar/2M\omega_\lambda}$ of the mode λ as $\delta_\lambda^{[i]} = \langle P_i^\dagger \Delta_\lambda P_i \rangle / \langle P_i \rangle$. We also define the distortion on site j due to the displaced modes when the electron is on site i as $u_j^{[i]} = \sum_\lambda \delta_\lambda^{[i]} V_\lambda(j)$. The dimerisation pattern $d_j^{[i]}$ is then calculated from $u_j^{[i]}$.

We plot on Fig. 3 the absolute value of the dimerisation $d_j^{[i]}$ from which the constant dimerisation d_c and the end effects have been subtracted (the corresponding pattern for the isolated molecule is shown on Fig. 2). Such a choice permits us to represent the defects with more contrast. For an injection energy $E = 0$ at mid-gap, the corresponding dimerisation is shown on Fig. 3(a). The bright feature around the middle of the chain represents the soliton. In the absence of e -ph coupling, this would correspond to charge injection in resonance with the one-electron soliton level (see the transmission curve below). The soliton would then be immobile, its position fixed in the middle of the chain and its width unchanged (*i.e.* straight vertical feature around $j = 50$). However due to the e -ph coupling, the soliton defect becomes mobile and its width varies while the electron propagates. Similar behaviour is observed for other injection energies around mid-gap. As E approaches the valence band edge the mechanisms become different, as shown on Fig. 3(b). In parallel with the soliton delocalization and deformation, one observes the formation of a polaron. This is characterized by the extra bright feature around the first

³ T_{ab} contains as usual the ratio of the velocity in the outgoing channel to that in the incoming channel.

⁴ The factors $v_{L,R}^2 / \beta_{L,R} \sin k_{b,a}^{L,R}$ in Eq.(2) are related to the imaginary parts of the potentials $\Sigma_{L,R}$.

⁵ Calculations were performed for an electron coupled to the $N_{\text{ph}} = 5$ lowest frequencies modes shown in Fig. 1 and $n_{\text{occ}}^{\text{max}} = 4$. Calculations were also done for other sets of parameters. The same qualitative physics remain when the results are converged versus the basis set size.

diagonal in Fig. 3(b). In principle, the (virtual) polaron corresponds to a local reduction of the dimerisation around the (tunneling) electron [16]. However it appears as an increase (positive number) since $|d_j^{[i]}|$ is plotted on Fig. 3(b). Furthermore, the corresponding dimerisation is not simply the superposition of the polaron and the soliton—the two defects interact strongly together. For example, the dimerisation pattern for an electron at position $i \approx 25$ is characteristic of a merging of both the polaron and soliton. Such mechanisms, leading to strong lattice distortions, would be expected to affect the transmission through the molecular wires—effects that we now consider.

We define an effective total transmission probability $T(E)$ arising from the contribution of the different outgoing channels as $T(E) \equiv \sum_a T_{ab}(\epsilon_{fin}, \epsilon_{in}) \delta(\epsilon_{fin} + \sum_\lambda n_\lambda \hbar\omega_\lambda - \epsilon_{in})$ (see Fig. 4). Without e -ph coupling, the transmission curve presents the usual features: resonances at energies corresponding to the one-electron levels of the molecule with almost perfect transmission, and strong suppression of the transmission in the band-gap of the molecule for which propagation occurs by tunneling. The soliton resonance (at mid-gap) is much narrower than the other resonances. This is to be expected since the corresponding one-electron (soliton) state is much more localized than the other states. With e -ph interaction, we have already shown that a polaron can be formed in the molecule and that the soliton position and width are strongly modified. Such mechanisms affect the transmission in the following way: (i) the delocalization and deformation of the soliton broaden but lower the resonance peak at mid-gap, (ii) for larger injection energies, the formation of the polaron effectively reduces the apparent band-gap, and a polaron resonance peak appears (at $E \approx 0.42$ eV for the $N = 99$ wire) inside the original gap. This effective band-gap reduction correlatively increases the transmission in the tunneling regime (*i.e.* for injection energies in the gap).

IV. CONCLUSION

The results presented above demonstrate the complexity of electronic transport through one-dimensional atomic-scale wires. We have illustrated the mechanisms of electron transport in molecular wires when e -ph interactions are included. Owing to e -ph coupling, polarons can be formed inside the molecule. Polaron propagation is the main mechanism of transport through perfectly dimerised (semiconducting) molecules. The presence of a mid-gap state associated to a soliton defect in the middle of the molecule involves different mechanisms for the transport. For injection energies around the mid-gap state, the delocalisation and deformation of the soliton is the main mechanism for electron transfer. With larger

injection energies (still inside the energy band-gap of the molecule), a virtual polaron can be formed. The transport is then associated with more complicated mechanisms involving the interaction of both polaron and soliton. However in most cases, the effective reduction of the band-gap due to polaron formation, the delocalization and deformation of the soliton and the polaron-soliton interaction increase the transmission in the tunneling regime. Although we studied a model derived from organic molecules, there is good reason to believe that the e -ph coupling in other one-dimensional nanoscale wires is likely to give rise to similar phenomena. In the case of carriers injected into dangling-bond lines on the Si(001) surface [2], polaron states which are in many respects analogous to those in molecular wires are also formed [23]. Specifically, we expect the present results to be valid for any atomic-scale wire in which there is a degeneracy between two different values of some order parameter (the dimerisation in the molecular case, the surface dimer buckling in the dangling bond line) which are related by a discrete symmetry and strongly coupled to the electrons.

ACKNOWLEDGMENTS

We acknowledge financial support from the U.K. EP-SRC (Grant GR/M09193).

-
- [1] van Wees B.J. *et al.*, Phys. Rev. Lett. **60** (1988) 848; Wharam D.A. *et al.*, J. Phys. C **21** (1988) L209.
 - [2] Hitosugi T. *et al.*, Phys. Rev. Lett. **82** (1999) 4034.
 - [3] Dong Z.C., Fujita D. and Nejh H., Phys. Rev. B **63** (2001) 115402.
 - [4] Lopinski G.P., Wayner D.D.M. and Wolkow R.A., Nature **406** (2000) 48.
 - [5] Costa-Krämer J.L. *et al.*, Phys. Rev. B **55** (1997) 5416.
 - [6] Ohnishi H., Kondo Y., and Takayanagi K., Nature **395** (1998) 780.
 - [7] Lemay S.G. *et al.*, Nature **412** (2001) 617.
 - [8] Reed M.A. *et al.*, Science **278** (1997) 252.
 - [9] Langlais V.J. *et al.*, Phys. Rev. Lett. **83** (1999) 2809.
 - [10] Donhauser Z.J. *et al.*, Science **292** (2001) 2303.
 - [11] Kergueris C. *et al.*, Phys. Rev. B **59** (1999) 12505.
 - [12] Tans S.J., Verschueren A.R.M., and Dekker C., Nature **393** (1998) 49.
 - [13] Dash L.K. and Fisher. A.J., J. Phys.: Condens. Matt. **13** (2001) 5035.
 - [14] Peierls R.E., *Quantum Theory of Solids* (Clarendon Press, Oxford) 1955.
 - [15] Heeger A.J. *et al.*, Rev. Mod. Phys. **60** (1988) 781.
 - [16] Ness H., Shevlin S.A. and Fisher A.J., Phys. Rev. B **63**

- (2001) 125422; Ness H. and Fisher A.J., Phys. Rev. Lett. **83** (1999) 452.
- [17] Samanta M.P. *et al.*, Phys. Rev. B **53** (1996) R7626; N. Lang and P. Avouris, Phys. Rev. Lett. **81**, 3515 (1998); Magoga M. and Joachim C., Phys. Rev. B **56** (1998) 4722.
- [18] Y. Lu, *Solitons and Polarons in Conducting Polymers*, (World Scientific, Singapore) 1988.
- [19] Chao K.A. and Wang Y., J. Phys. C **18** (1985) L1127.
- [20] Bonča J. and Trugman S.A., Phys. Rev. Lett. **75** (1995) 2566; **79** (1997) 4874.
- [21] Sols F., Ann. Phys. **214** (1992) 386.
- [22] Xie S. and Mei L., Phys. Rev. B **47** (1993) 14905; Sun X. *et al.*, Phys. Rev. B **35** (1987) 4102.
- [23] Bowler D.R. and Fisher A.J., Phys. Rev. B **63** (2001) 035310.

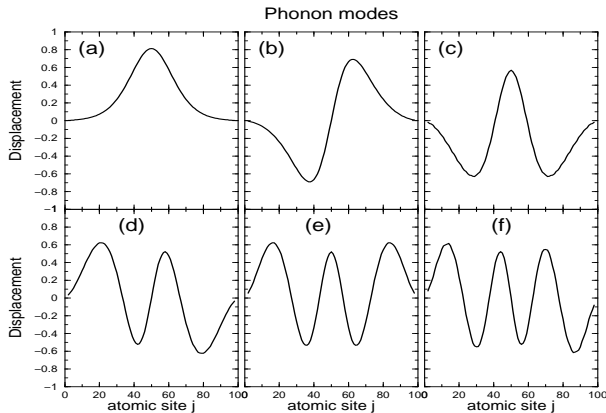


FIG. 1. Optic component of the phonon modes for a chain length $N = 99$. The optic component is defined as: $(-1)^j(V_\lambda(j+1) - 2V_\lambda(j) + V_\lambda(j-1))$. (a) is the mode associated with the soliton translation ($\hbar\omega_a=0.020$ eV), (b) with the deformation of the soliton width ($\hbar\omega_b=0.114$ eV), (c) is the so-called third mode ($\hbar\omega_c=0.134$ eV). (d,e,f) are other long-wavelength optic modes ($\hbar\omega_{d,e,f}=0.144, 0.152, 0.158$ eV).

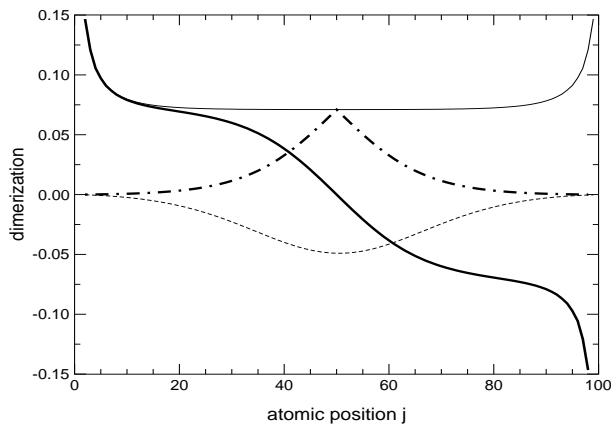


FIG. 2. Dimerisation d_j (in Å) for isolated neutral molecules. *Thin solid line*: $N = 100$, for even N , d_j is constant (d_c) in the middle of the chain. *Solid line*: $N = 99$, for odd N , a soliton exists in the middle of the chain separating two domains of dimerisation with opposite site. *Dot-dashed line*: the absolute value $|d_j|$ from which d_c and the end effects are subtracted ($N = 99$). *Thin dashed line*: deformation induced by adding an extra electron in the chain $N = 100$; the local reduction of the dimerisation represents a polaron.

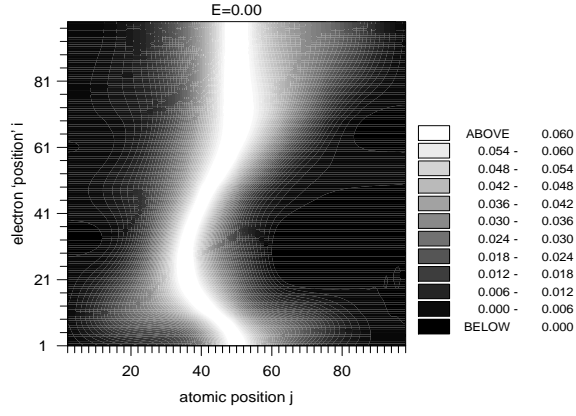


Fig. 3(a)

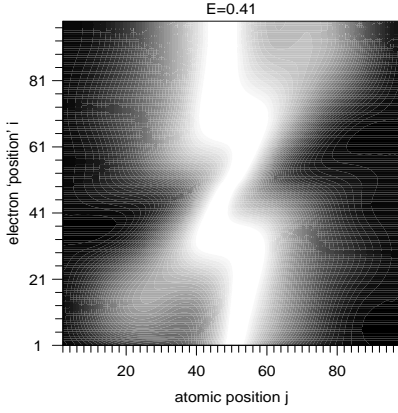


Fig. 3(b)

FIG. 3. Two-dimensional (atomic j /electron i positions) map of the dimerisation $d_j^{[i]}$ (in Å) obtained from the atomic distortions $u_j^{[i]}$ for the $N = 99$ wire length. Here we plot the absolute value $|d_j^{[i]}|$ subtracting d_c and the end effects. The incoming electron propagates from the left to the right. (a) Injection at mid-gap ($E = 0.0$): the bright feature represents the soliton whose position and width vary for the different electron positions i taken to calculate $d_j^{[i]}$. (b) Injection at $E = 0.41$ eV close the polaron resonance peak in the transmission (Fig. 4): a virtual polaron is formed (bright feature across the first diagonal). The maximum change in $|d_j^{[i]}|$ is $\approx 0.03 - 0.04$ Å around the polaron and ≈ 0.07 Å around the soliton.

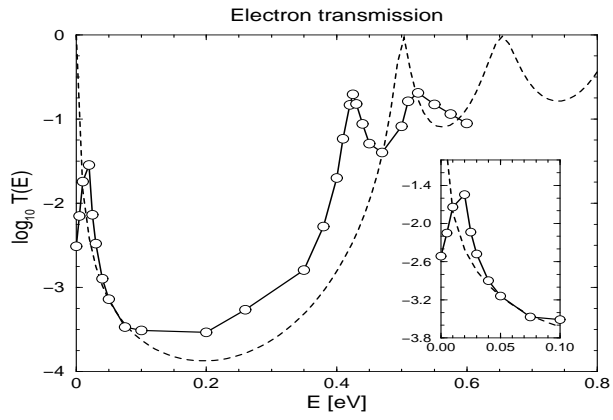


FIG. 4. Transmission probability $T(E)$ versus the energy E for a molecular wire of length $N = 99$. *Dashed line*: transmission through a rigid chain containing a soliton defect (see the sharp peak at $E = 0$ corresponding to the soliton state resonance). *Solid line with circles*: transmission when the e -ph coupling is included. The delocalisation of the soliton and the polaron-soliton interaction broaden the resonance peak at mid-gap into a “mini-band” (shown in the inset, enlarged low-energy region). The polaron resonance peak appears around $E \approx 0.42$ eV.